Saudi Pharmaceutical Journal 25 (2017) 575–579

Contents lists available at ScienceDirect

Saudi Pharmaceutical Journal

journal homepage: www.sciencedirect.com

Original article

Osteogenic differentiation of bone marrow mesenchymal stem cells by magnetic nanoparticle composite scaffolds under a pulsed electromagnetic field

Jianghong Huang [a,b,c], Daming Wang [a,b,c,d], Jielin Chen [a,b,c], Wei Liu [a,b,c], Li Duan [a,b,c], Wei You [a,b,c], Weimin Zhu [a,b,c], Jianyi Xiong [a,b,c], Daping Wang [a,b,c,*]

[a] Shenzhen National Key Department of Orthopedics, Shenzhen Second People's Hospital, Shenzhen 518035, China
[b] Shenzhen Key Laboratory of Tissue Engineering, Shenzhen Second People's Hospital, Shenzhen 518035, China
[c] Shenzhen Laboratory of Digital Orthopedic Engineering, Shenzhen Second People's Hospital, Shenzhen 518035, China
[d] Software Town of Shenzhen Universiade, Shenzhen Longer3d Technology, Shenzhen 518116, China

ARTICLE INFO

Article history:
Available online 8 May 2017

Keywords:
Magnetic nanoparticles
Bone marrow mesenchymal stem cells
Osteogenic differentiation
Pulsed electromagnetic field

ABSTRACT

This study was conducted to investigate the effect of magnetic nanoparticle composite scaffold under a pulsed electromagnetic field on bone marrow mesenchymal stem cells (BMSCs), which was achieved by examining the biological behaviors of cell adhesion, proliferation and differentiation on the surface of the scaffolds. This may provide some experimental evidence for the use of magnetic nanoparticles in medical application. The magnetic nanoparticle composite scaffolds were evaluated and characterized by the following indexes: the cell proliferation was detected by the CCK-8 method, the alkaline phosphatase (ALP) activity was examined by a detection kit, and the expression of type I collagen and osteocalcin gene were evaluated by RT-PCR. The CCK-8 test showed that there was no significant difference in Group A (BMSCs-seeded magnetic scaffolds under the electromagnetic field), B (BMSCs-seeded magnetic scaffolds) and C (BMSCs cultured alone) ($P > 0.05$). The value for the ALP activity in Group A was higher than the other two groups. In addition, the RT-PCR results showed that the expression of type I collagen gene in Group A was enhanced ($P < 0.05$), suggesting that the magnetic nanoparticles combined with the pulsed electromagnetic field had a positive effect on the osteogenic differentiation of BMSCs. However, the expression of osteocalcin was not significantly different in three groups ($P > 0.05$). To conclude, magnetic nanoparticles may induce the osteogenic differentiation with the action of the pulsed electromagnetic field.
© 2017 The Authors. Production and hosting by Elsevier B.V. on behalf of King Saud University. This is an open access article under the CC BY-NC-ND license (http://creativecommons.org/licenses/by-nc-nd/4.0/).

1. Introduction

In recent years, with the development of bioengineering and biomedicine, some functional molecules of medical drugs have been introduced to improve biomedical materials (Nawaz et al., 2017). Magnetic nanoparticles have attracted much attention as a new medical drug in the biomedical field, and are widely applied in targeting delivery, bio-imaging and cancer therapy (Weizenecker et al., 2009; Wang et al., 2013; Maleki-Ghaleh et al., 2016; Hu et al., 2009; Hirsch et al., 2003). The most unique feature of magnetic nanoparticles is the response to the electromagnetic field, enabling some applications such as drug targeting and the separation of molecules and cells (Son et al., 2005). Moreover, the electromagnetic field can exert the appropriate force on the cells with magnetic particles, offering a powerful tool to control cell behaviors. For example, Bradshaw et al. (2015) found that the migration speed of fibroblasts can be enhanced with the internalized magnetic nanoparticles in the presence of a electromagnetic field. Perica et al. (2014) showed that T cell receptor antibody immobilized paramagnetic particles could bind to cell surface and formed large agglomerates under the electromagnetic field, leading to the receptors binding to each other and thus the activation of specific cell functions. Jiang et al. (2016) also showed that bone marrow mesenchymal stem cells can differentiate into osteoblasts under the action of magnetic nanoparticles and the

* Corresponding author at: Shenzhen National Key Department of Orthopedics, Shenzhen Second People's Hospital, Shenzhen 518035, China.
E-mail address: dapingwang1963@qq.com (D. Wang).
Peer review under responsibility of King Saud University.

Production and hosting by Elsevier

http://dx.doi.org/10.1016/j.jsps.2017.04.026
1319-0164/© 2017 The Authors. Production and hosting by Elsevier B.V. on behalf of King Saud University.
This is an open access article under the CC BY-NC-ND license (http://creativecommons.org/licenses/by-nc-nd/4.0/).

external electromagnetic field, and promoted the expression of osteocalcin and type I collagen. It is thus believed that the force generated by the magnetic nanoparticles under a electromagnetic field will influence cell behaviors significantly. In this study, magnetic nanoparticle composite scaffolds were prepared using the magnetic nanoparticles Fe_2O_3, Nano-hydroxyapatite (n-HA) and L-polylactic acid (PLLA). *In vitro* study of BMSCs seeded onto the magnetic nanoparticle composite scaffolds under a pulsed electromagnetic field was performed, which was to explore the cell adhesion, proliferation, differentiation and other biological behaviors in this case. This may provide some experimental evidence for the use of magnetic nanoparticles in medical application (Gohar et al., 2017; Muhammad et al., 2017).

2. Material and methods

2.1. Experimental materials and instruments

Fe_2O_3, n-HA and PLLA were obtained from Shandong Medical Instruments Institute, China. α-MEM, fetal bovine serum, 500 U/mL penicillin and 500 μg/mL streptomycin were purchased from Gibco, USA. CCK-8 cell proliferation and alkaline phosphatase detection kit were obtained from Keygen, China. TRIzol®Reagent was purchased from Invitrogen, USA. A low temperature rapid prototyping instrument (Shenzhen Institute of Advanced Technology, Chinese Academy of Sciences, China) was used for the fabrication of magnetic nanoparticle composite scaffolds. SEM imaging was conducted using a scanning electron microscopy (MIRA3 TESCAN, Tsinghua University, Shenzhen Institute, China). Pulsed electromagnetic field was obtained from a CLM-B-type pulse magnetic field therapy instrument (Hebei Langfang Hammer Medical Devices Company, China).

2.2. Fabrication of magnetic nanoparticle composite scaffolds

Fe_2O_3, n-HA and PLLA were mixed into an aqueous solution in a certain mass ratio, and the magnetic nanoparticle composite scaffolds were prepared using low-temperature rapid prototyping (Fig. 1a). The scaffold is a three-dimensional porous structure with a porosity of 80–85%. The SEM image shows that the pores are highly interconnected. At a higher magnification, the surface of the scaffold is uneven with the magnetic nanoparticles evenly distributed on the surface (Fig. 1b). Prior to the cell test, magnetic nanoparticle composite scaffolds were processed with the ultraviolet radiation for half an hour, followed by soaking in the PBS solution for cleaning and the 75% ethanol disinfection.

2.3. Isolation and culture of bone marrow mesenchymal stem cells (BMSCs)

3 months old New Zealand white rabbits were routinely anaesthetized, disinfected, and left femur trochanter. Bone marrow was aspirated with a 2 mL heparin syringe and placed in a 10 mL centrifuge tube with 5 mL PBS solution, followed by a 1200 r/min centrifugation for 10 min. High glucose DMEM medium (containing 10% FBS, 1% double antibody (penicillin/streptomycin)) was added to the cell suspension after removing the supernatant, which was then incubated with 5% CO_2 at 37 °C. At 80% confluency, BMSCs were harvested by trypsin, suspended in DMEM, centrifuged, and diluted to a concentrated cell suspension. Medium was changed every 3 days by removing 1 mL and replenishing 1 mL. BMSCs were spindle, triangular or irregular polygon under the microscope (Fig. 2).

2.4. BMSCs-seeded magnetic nanoparticle composite scaffolds

In this study, three groups were divided: In Group A and Group B, BMSCs (1×10^5 cells) were seeded on the magnetic nanoparticle composite scaffolds and were inoculated into a-MEM medium containing 10% fetal bovine serum under the aseptic condition (Fig. 3a). A pulsed electromagnetic field with the magnetic field strength of 100MT was applied in Group A (Fig. 3b). In Group C BMSCs (1×10^5 cells) were cultured alone. All the groups were placed in the 37 °C incubator supplied with 5% CO_2. The media were refreshed every 3 days.

2.5. Detection of cell proliferation activity

A Cell Counting Kit-8 (CCK-8) method was applied to the three groups. In each group, 50 μL of CCK-8 solution was added at 1, 3, 7, 14 and 21 days of cell culture (n = 5), which was incubated with the samples at 37 °C for 4 h. The light absorption value (A value) was obtained at 490 nm using a microplate reader to plot the cell proliferation curve.

2.6. Alkaline phosphatase (ALP) quantification

ALP is an early stage marker of osteogenic differentiation of BMSCs, which is elevated at relative early days and decreased at later stage. Therefore Day 7 was selected as the time point to check

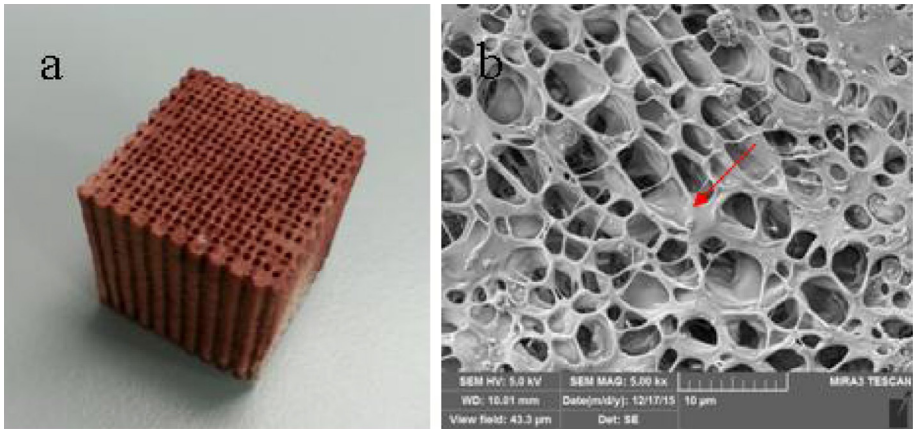

Fig. 1. (a) Magnetic nanoparticle composite scaffold (gross view) and (b) the microstructure of magnetic nanoparticle composite scaffold (SEM), the surface of the scaffold is uneven with the magnetic nanoparticles evenly distributed on the surface.

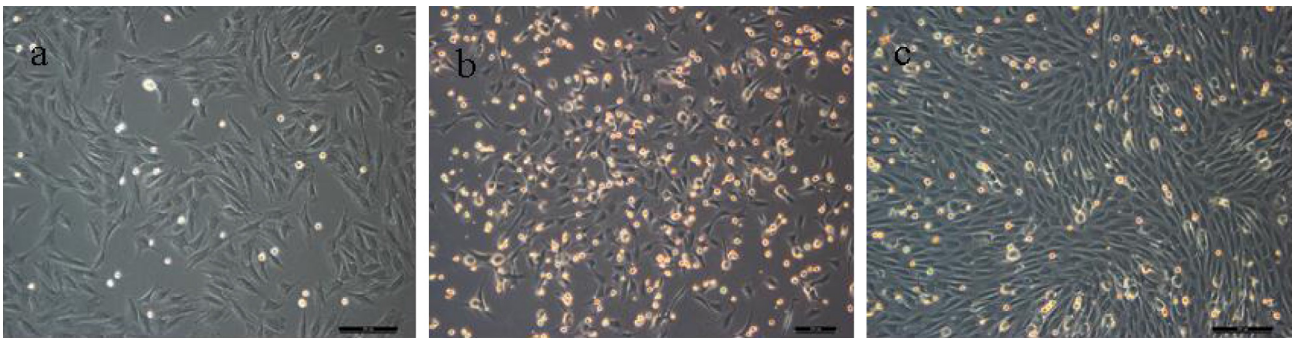

Fig. 2. BMSCs were spindle, triangular or irregular polygon under the microscope. From (a) to (c): P0, P1, P3. Scale bar is 100 μm.

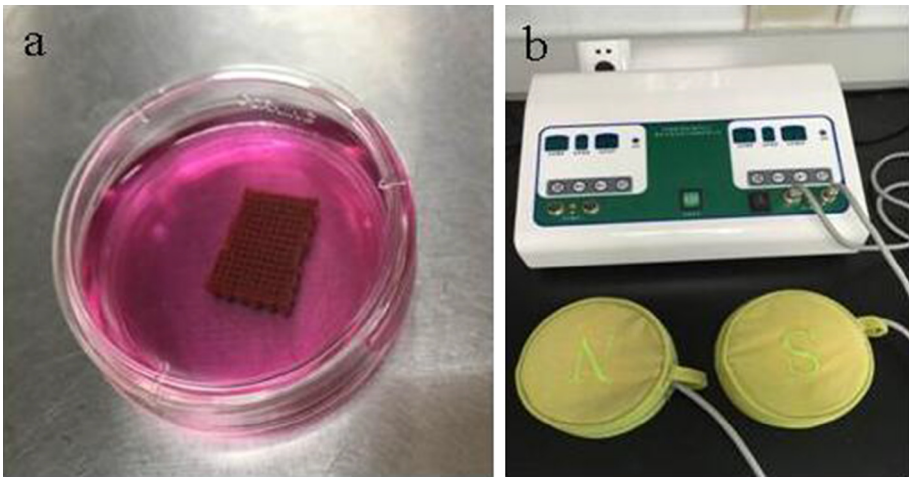

Fig. 3. (a) BMSCs-seeded magnetic nanoparticle composite scaffolds and (b) the pulsed magnetic field therapy instrument.

the ALP expression. MSCs were washed with PBS for 3 times and treated with 0.5% Triton/PBS at 4 °C for 24 h. After ALP was totally released, the solution was mixed with reagents from the colorimetric Kit. The absorbance at 490 nm was recorded by a microplate reader, and the activity of ALP was calculated by referring to a calibration curve. The ALP activity per 10^4 cells was reported.

2.7. Expression of COL I and OCN

According to Sagomonyants et al. (2011), BMSCs were cultured for 21 days and 1×10^6 cells were collected. Total RNA extraction was performed using 1 mL of TRIzol (Invitrogen). The extracted RNA was quantified by absorbance and was measured with a UV spectrophotometer (WPA UV1101), with A260/280 > 1.8. A two-step RT-PCR detection was performed. The method and conditions of the first-strand cDNA synthesis conformed to the instruction on the assay kit (Fermentas). The 25 μL reaction system consisted of 2.5 μL of 10 × Taq buffer, 3.0 μL of 25 mmol/L $MgCl_2$, 2.0 μL of 10 mmol/L dNTP, 1.0 μL of Taq DNA polymerase (1 U/μL), 18.5 μL of ddH20, 1.0 μL of template cDNA and 1.0 μL each of forward primer and reverse primer (20 μL). The PCR program was as follows: predenaturation at 95 °C for 3 min, 1 cycle; annealing for 45 s (see the annealing temperature below), extension at 72 °C for 1 min, 30 cycles, and extension at 72 °C for 7 min. Type I collagen (COL I), upstream primer 5′-CACTGGCGATAGTGGTCCTG-3′, downstream primer 5′-CGGCCACCA TCTTGAGACTT-3′, annealing temperature 53 °C, amplified fragment 132 bp; OCN, upstream primer 5′-TGCC AGGTCACCAAATACCA-3′, downstream primer 5′-TGAGTACTGA GAGGCCCCAA-3′, Annealing temperature 58 °C, amplified fragment 112 bp; reference β-actin, upstream primer 5′-TGAGACCTT CAACACCCC-3′, downstream primer 5′-GCCATCTCTTGCTC GAAGTC-3′, annealing temperature 56 °C, amplified fragment 316 bp . Next, 5 μL of products amplified using the primers of COL I, OCN and β-actin were stained by GelRed and treated with 2% agarose gel electrophoresis, respectively. The gray scales of different bands were measured with the Quantity One software, and semi-quantitative analysis was performed.

2.8. Statistical analysis

The measurement data were expressed as $x \pm s$. One way ANOVA was carried out for each group of data using SPSS 13.0. For intergroup comparison, the SNK-q test was performed.

3. Results and discussion

3.1. Cell proliferation

The proliferation curve of BMSCs regarding the three groups is shown in Fig. 4. There was no significant difference in the cell proliferation between Group A, B and C ($P > 0.05$). From the proliferation curve we can see that the cells from the three groups in the 21-day proliferation period had a similar proliferation trend, indicating that the addition of magnetic nanoparticles and the usage of the pulsed electromagnetic field showed less effect on the cell compatibility.

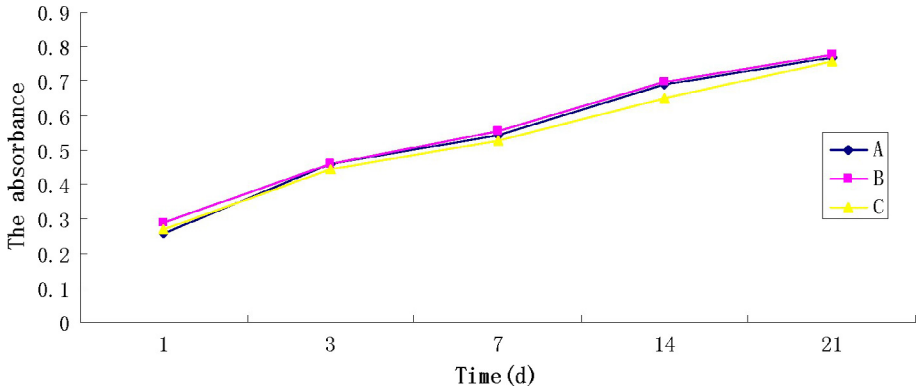

Fig. 4. CCK-8 assay, showing no significant difference in the cell proliferation between Group A, B and C ($P > 0.05$).

3.2. ALP quantification

ALP is an important osteogenic marker at the earlier stage of osteogenesis differentiation of BMSCs (Zhu et al., 2013), the alkaline phosphatase assay was used to detect the ALP activity. Fig. 5 showed that the value for the activity of ALP in Group A was the highest. This suggested that the magnetic nanoparticles combined with the pulsed electromagnetic field had a positive effect on the osteogenic differentiation of BMSCs (Zaidi et al., 2017; Samad et al., 2017).

3.3. RT-PCR detection of the expression of COL I and OCN

COL I and OCN are both important osteogenic differentiation hallmarks at relatively later stage. It has been proved that COL I is the most abundant protein in the organic/inorganic composite matrix of bone tissue (Zhu et al., 2013; Ding et al., 2016). OCN is the most abundant noncollagenous protein in the bone matrix, which plays an essential role in bone formation and remodeling (Nakamura et al., 2009; Wang, 2016). Here the expression of COL I and OCN were studied in the gene level. In Group A, the expression of COL I had a significant increase compared to the other two groups after 21 days of cell culture (Fig. 6, $P < 0.05$). However, the expression of OCN was not significantly different in the three groups ($P > 0.05$), as shown in Fig. 6.

To conclude, the experimental results showed that magnetic nanoparticle combined with the pulsed electromagnetic field synergistically promoted the osteogenesis of BMSCs, suggesting a potential biomedical application for bone tissue engineering. Indeed, by combinational applications of electromagnetic field and magnetic particles to cells, many cell functions such as migration, angiogenesis, ion channel activation and even apoptosis can be regulated (Creixell et al., 2011; Zhang et al., 2014; Cho et al., 2012; Lee et al., 2010; Zaheer et al., 2017). However, the differentiation of stem cells is still not tacked up to present. In this study, we present the potential to induce the osteogenic differentiation of BMSCs by using magnetic particles and the pulsed electromagnetic field. Fe_2O_3 is a kind of magnetic nanoparticles, which has the magnetic response and superparamagnetism. It can be aggregation and positioning in a pulsed electromagnetic field, and be absorption of electromagnetic wave heat in the alternating pulsed electromagnetic field. Since the magnetic nanoparticles have the ability to bind to the cell surface, this makes it possible to control and regulate the function of the cells under the applied pulsed electromagnetic field. The cell proliferation results indicate that magnetic nanoparticles can be used as a medical molecular with good cell compatibility. Therefore our findings convey the significance of evaluating the safety issue of magnetic nanoparticles under the pulsed electromagnetic field.

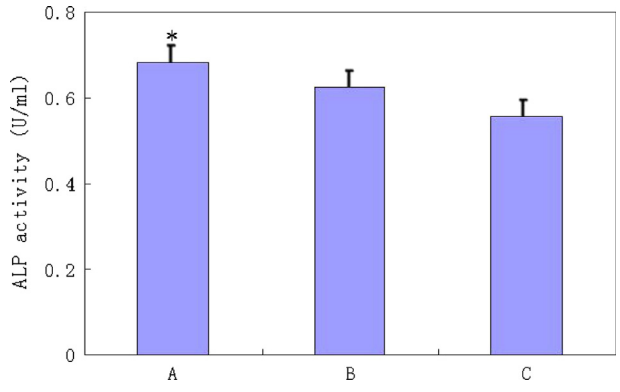

Fig. 5. ALP activity of the three groups, the value for Group A was the highest and the results were significantly different ($P < 0.05$).

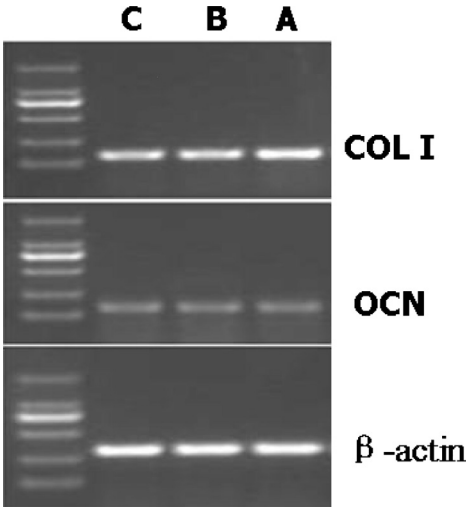

Fig. 6. RT-PCR results showing the expression of COL I ($P < 0.05$) and osteocalcin (OCN, $P > 0.05$) after 21 days of cell culture. β-actin was the internal reference primers. The expression of COL I was significantly different in the three groups.

4. Conclusions

In this study, there was no significant difference ($P > 0.05$) in the three groups regarding the rate of cell proliferation, suggesting the addition of magnetic nanoparticles and the usage of the pulsed electromagnetic field showed less effect on the cell compatibility.

In terms of the ALP activity, the value of Group A was higher than the other two groups. In addition, the expression of COL I in Group A increased significantly ($P < 0.05$), implying that the magnetic nanoparticles combined with the pulsed electromagnetic field had the positive effect on the osteogenic differentiation of BMSCs. However, the expression of OCN had no significant difference in three groups ($P > 0.05$). The experimental results showed that magnetic nanoparticle under the pulsed electromagnetic fields synergistically promoted the osteogenesis of BMSCs, which may be a potential biomedical application for bone tissue engineering.

Acknowledgements

This study was mainly supported by Grants from: National Natural Science Foundation of China (No. 51603125), Natural Science Foundation of Guangdong Province, China (No. 2016A030310030), Shenzhen R & D funding project (No. CXZZ20140813160132596, No. JCYJ20160301111338144), Shenzhen Medical Science Foundation (No. 201605005) and Fund for High Level Medical Discipline Construction of Shenzhen (No. 2016031638).

References

Bradshaw, M., Clemons, T.D., Ho, D., et al., 2015. Manipulating directional cell motility using intracellular superparamagnetic nanoparticles. Nanoscale 7, 4884–4889.

Cho, M.H., Lee, E.J., Son, M., et al., 2012. A magnetic switch for the control of cell death signalling in in vitro and in vivo systems. Nat. Mater. 11, 1038–1043.

Creixell, M., Bohorquez, A.C., Torres-Lugo, M., Rinaldi, C., 2011. EGFR-targeted magnetic nanoparticle heaters kill cancer cells without a perceptible temperature rise. ACS Nano 5, 7124–7129.

Ding, Y.Q. et al., 2016. Stress analysis and creep life prediction of hydrogen reformer furnace tube. J. Mech. Eng. Res. Develop. 39 (3), 744–756.

Gohar, S., Abbas, G., Sajid, S., Sarfraz, M., Ali 1, S., Ashraf, M., Aslam, R., Yaseen, K., 2017. Prevalence and antimicrobial resistance of Listeria monocytogenes isolated from raw milk and dairy products. Matrix Sci. Medica 1 (1), 10–14.

Hirsch, L.R., Stafford, R., Bankson, J., et al., 2003. Nanoshell-mediated near-infrared thermal therapy of tumors under magnetic resonance guidance. Proc. Natl. Acad. Sci. 100, 13549–13554.

Hu, L., Mao, Z., Gao, C., 2009. Colloidal particles for cellular uptake and delivery. J. Mater. Chem. 19, 3108–3115.

Jiang, P., Zhang, Y., Zhu, C., Zhang, W., Mao, Z., Gao, C., 2016. Fe3O4/BSA particles induce osteogenic differentiation of mesenchymal stem cells under static magnetic field. Acta Biomater. http://dx.doi.org/10.1016/j.actbio.2016.09.020.

Lee, J.H., Kim, E.S., Cho, M.H., et al., 2010. Artificial control of cell signaling and growth by magnetic nanoparticles. Angew. Chem. Int. Ed. 49, 5698–5702.

Maleki-Ghaleh, H., Aghaie, E., Nadernezhad, A., et al., 2016. Influence of Fe_3O_4 nanoparticles in hydroxyapatite scaffolds on proliferation of primary human fibroblast cells. JMEPEG 25, 2331–2339.

Muhammad, G., Rashid, I., Firyal, S., 2017. Practical aspects of treatment of organophosphate and carbamate insecticide poisoning in animals. Matrix Sci. Pharma 1 (1), 10–11.

Nakamura, A., Dohi, Y., Akahane, M., et al., 2009. Osteocalcin secretion as an early marker of in vitro osteogenic differentiation of rat mesenchymal stem cells. Tissue Eng. Part C Meth. 15, 169–180.

Nawaz, S., Shareef, M., Shahid, H., Mushtaq, M., Sajid, S., Sarfraz, M., 2017. Lipid lowering effect of synthetic phenolic compound in a high- fat diet (HFD) induced hyperlipidemic mice. Matrix Sci. Pharma 1 (1), 12–16.

Perica, K., Tu, A., Richter, A., Bieler, J.G., Edidin, M., Schneck, J.P., 2014. Magnetic fieldinduced T cell receptor clustering by nanoparticles enhances T cell activation and stimulates antitumor activity. ACS Nano 8, 2252–2260.

Sagomonyants, K.B., Hakim-Zargar, M., Jhaveri, A., et al., 2011. Porous tantalum stimulates the proliferation and osteogenesis of osteoblasts from elderly female patients. J. Orthop. Res. 4, 609–616.

Samad, A.N.S., Amid, A., Jimat, D.N., Shukor, A.N.A., 2017. Isolation and identification of halophilic bacteria producing halotolerant protease. Galeri Warisan Sains 1 (1), 07–09.

Son, S.J., Reichel, J., He, B., Schuchman, M., Lee, S.B., 2005. Magnetic nanotubes for magnetic-field- assisted bioseparation, biointeraction, and drug delivery. J. Am. Chem. Soc. 127, 7316–7317.

Wang, M., Li, Z., Qiao, H., Chen, L., Fan, Y., 2013. Effect of Gold/Fe_3O_4 nanoparticles on biocompatibility and neural differentiation of rat olfactory bulb neural stem cells. J. Nanomater. 867426, 7.

Wang, H.D., 2016. Evaluating energy consumption and performance of centrifugal water chillers with few field data. J. Mech. Eng. Res. Develop. 39 (4), 953–968.

Weizenecker, J., Gleich, B., Rahmer, J., Dahnke, H., Borgert, J., 2009. Three-dimensional real-time in vivo magnetic particle imaging. Phys. Med. Biol. 54, L1.

Zaheer, Z., Rahman, U.S., Zaheer, I., Abbas, G., Younas, T., 2017. Methicillin-resistant Staphylococcus aureus in poultry – an emerging concern related to future epidemic. Matrix Sci. Med. 1 (1), 15–18.

Zaidi, N.A., Hamid, A.A.A., Hamid, T.A.T.H., 2017. Lactic acid bacteria with antimicrobial properties isolated from the instestines of Japanese quail (Coturnix Coturnix Japonica). Galeri Warisan Sains 1 (1), 10–12.

Zhang, E., Kircher, M.F., Koch, M., Eliasson, L., Goldberg, S.N., Renström, E., 2014. Dynamic magnetic fields remote-control apoptosis via nanoparticle rotation. ACS Nano 8, 3192–3201.

Zhu, Y., Mao, Z., Gao, C., 2013. Control over the gradient differentiation of rat BMSCs on a PCL membrane with surface-immobilized alendronate gradient. Biomacromolecules 14, 342–349.